Statistics on Anatomic Objects Reflecting Inter-Object Relations

Ja-Yeon Jeong, Stephen M. Pizer, Surajit Ray

Statistics on Anatomic Objects Reflecting Inter-Object Relations

Ja-Yeon Jeong, Stephen M.Pizer, and Surajit Ray

Medical Image Display & Analysis Group (MIDAG)
University of North Carolina, Chapel Hill NC 27599, USA

Abstract. Describing the probability densities of multi-object complexes by describing individual objects and their inter-object relationships leads to desirable locality without ignoring the context of an object. We describe a means of decomposing object variations into self effects and neighbor effects. We describe an approach for estimating the self and neighbor effect probability densities for each object in the complex using augmentation and prediction, supported by PGA on m-reps. We apply this method to the inter-day variation of m-reps of male pelvic organs within an individual patient.

1 Introduction

Statistical shape models have been proven to be very effective in a number of applications, including image segmentation [1] and characterization of the anatomic differences between the classes of normal and diseased patients [2]. In segmentation, prior shape statistics restrict the deformation of the shape model within the variations learned from training data in this optimization process. In characterization of anatomic differences these statistics provide the basis for a test of a null hypothesis that the probability densities for the two classes are the same. Obtaining accurate shape statistics is thus essential.

Shape statistics are likely to be more sensitive measures when multiple objects in a given anatomic region are considered since frequently the intensity information does not fully provide the boundary of a target object without considering the neighbors that provide its context.

Following the approach that others have taken, we have calculated both global statistics on combined shape models of the multiple objects and statistics on each object separately. We found that the former approach fails to capture the local variation of an object itself and sometimes gives misleading information about inter-relation between objects. The latter approach gives too local information while ignoring the interaction between objects. The weakness of both approaches has led us to borrow the idea of the mixed model [3] approach to handle the inter-object relation. In this work we decompose the shape variation of each of the objects into three components: the mean of the variation from some base state, self effects, and neighbor effects. The neighbor effects term are described as a function of neighbors' geometric descriptors since shape variations of an object closely surrounded by other objects are caused not only by

internal changes within the object but also by its neighboring objects. The self term describes the variation of the object itself, not affected by its neighboring objects. We present in this paper an approach to estimate probability densities on each of these components individually.

We use a single-figure m-rep model [1] for each object as the shape representation. M-reps consist of sheets of medial atoms. Medial atoms capture not only local position but also the local orientation and local magnification of a section of an object. M-reps also provide correspondences across cases of the object derived from the local coordinate system for object interiors that m-rep provides. Therefore, m-reps are powerful representation to characterize the neighbor relationship, allowing medial atoms in neighboring objects to be understood in terms of atom transformations of each other.

For both the self and neighbor terms we estimate probability densities on the nonlinear manifold by a method called principal geodesic analysis (PGA) developed in our previous work [4]. The approach for the neighbor term is an extension of our earlier work [5], [13] in which an augmentation and prediction method is introduced to estimate the relation among multiple objects.

Section 2 describes other approaches in estimating multi-object geometric statistics and basic ideas of residues, augmentation, and prediction. The difference and addition operations through which residues are obtained are also explained in that section. Section 3 presents our new iterative method to estimate self and neighbor effects of multi-objects with mathematical detail. Section 4 explains the process to estimate these probability densities for the male-pelvis data to which we applied our new method, and it gives the results of the estimation. Section 5 discusses the results as well as the work yet to be done.

2   Background

Multi-object shape statistics in deformable template models has been mostly dealt with by doing global statistics on all objects taken together. This approach has been applied on a variety of shape representations: point distribution models [6], diffeomorphisms from atlases [7], distance functions or their levels sets [8], and m-reps [1]. This global statistics lacks appropriate locality of the objects.

Other approaches in doing shape statistics have handled locality, addressing the issue of scale. They compute shape statistics hierarchically from the object complex to the individual objects [9], [10], and one of these even analyzes residues from a larger scale [11]. However, few attempts have been made to describe the inter-object relation statistically. Pohl et al. [12] describes inter-relationships by representing via the distance function to objects' boundaries. This approach however does not explicitly separate out inherent variation of object from the effects from its neighbor.

In this work we do not consider a global stage since our target problem appears to have only single object effects and inter-object effects. However, we do decompose the objects' variation into self and neighbor effects, which must sum to the overall difference of the object from its base state. Thus the self

effect must be the residue describing overall change from the base state after the neighbor effect is removed, and the neighbor effect must be the residue describing overall change from the base state after the self effect is removed. This explicit separation between self and neighbor variation is the main improvement that we have made on our earlier method [5]. We rely on the difference operation $\ominus$ on m-reps to obtain the residue. The difference operation and its complementary addition operation are described briefly in the next.

A medial atom $\underline{\mathbf{m}} = (\mathbf{x}, r, \mathbf{u}, \mathbf{v})$ is defined as an element of the symmetric space $G = R^3 \times R^+ \times S^2 \times S^2$ where the hub position $\mathbf{x} \in R^3$, the spoke length $r \in R^+$, and the two unit spoke directions $\mathbf{u}, \mathbf{v} \in$ the unit sphere S^2. Let $\mathbf{R_w}$ represent the rotation along the geodesics in S^2 that moves a point $\mathbf{w} \in S^2$ to the north pole $\mathbf{p} = (0, 0, 1) \in S^2$. For given any two medial atoms $\underline{\mathbf{m}}_1, \underline{\mathbf{m}}_2 \in G$ where $\underline{\mathbf{m}}_i = (\mathbf{x}_i, r_i, \mathbf{u}_i, \mathbf{v}_i), i = 1, 2$, the difference between them can be described as follows:

$$\underline{\mathbf{m}}_1 \ominus \underline{\mathbf{m}}_2 := (\mathbf{x}_1 - \mathbf{x}_2, \tfrac{r_1}{r_2}, \mathbf{R}_{\mathbf{u}_2}(\mathbf{u}_1), \mathbf{R}_{\mathbf{v}_2}(\mathbf{v}_1)) \ . \tag{1}$$

Its corresponding addition operator $\oplus$ is thus defined as

$$\underline{\mathbf{m}} \oplus \Delta\underline{\mathbf{m}} := (\mathbf{x} + \Delta\mathbf{x}, r \cdot \Delta r, \mathbf{R}_{\mathbf{u}}^{-1}(\Delta\mathbf{u}), \mathbf{R}_{\mathbf{v}}^{-1}(\Delta\mathbf{v})) \tag{2}$$

for a given $\underline{\mathbf{m}} = (\mathbf{x}, r, \mathbf{u}, \mathbf{v})$ and difference $\Delta\underline{\mathbf{m}} = (\Delta\mathbf{x}, \Delta r, \Delta\mathbf{u}, \Delta\mathbf{v})$. For two m-reps $\underline{\mathbf{M}}_1, \underline{\mathbf{M}}_2$ that consist of medial atoms, the difference $\underline{\mathbf{M}}_1 \ominus \underline{\mathbf{M}}_2$ relative to $\underline{\mathbf{M}}_2$ coordinate is thus defined as the collection of the differences of corresponding individual atoms in two m-reps. These operations and their properties are explained in detail in [13].

We also extend the augmentation and prediction methods described in [5]. We make use of augmentation to deal with a target object's inter-relation with other objects. Based on the evidence that atoms in a target object are highly correlated with abutting atoms in the neighboring objects, we choose a set of atoms $\underline{\mathbf{A}}$ in the target object that are located near its neighboring objects and a set of atoms $\underline{\mathbf{N}}$ in neighboring objects that are close to $\underline{\mathbf{A}}$. We then produce the augmented set of atoms by putting atoms in $\underline{\mathbf{N}}$ and $\underline{\mathbf{A}}$ together into one set of atoms $\underline{\mathbf{U}}$. This augmentation allows us predict the changes brought on a target object by the change of the neighboring objects, namely as the mean of its $\underline{\mathbf{A}}$ conditioned on its neighbor atoms $\underline{\mathbf{N}}$. Then we can statistically analyze variations from this prediction. This prediction method helps to extract the deterministic effect from its neighbor on the object and concentrate on the variable part in the neighbor effects. A major improvement on our earlier method is that we consider the neighbor relation mutually, allowing each object to have any of the others as neighbors. This mutual neighbor relation is more realistic and is clearly suggested in the male-pelvis data to which we apply our new method.

3   Method in detail

Let $\Delta\underline{\mathbf{M}}^i := \underline{\mathbf{M}}^i \ominus \underline{\mathbf{M}}^b$ where $\underline{\mathbf{M}}^b$ is a base model such as the mean or some reference model, where i indexes the training cases and $\underline{\mathbf{M}}$ represents an m-rep.

All figures in $\underline{\mathbf{M}}^i$ are aligned to figures in the base model. $\{\Delta\underline{\mathbf{M}}^i\}$ are variations of m-reps from the base m-rep model. We decompose the variations into two parts, *self* and *neighbor*, as follows:

$$\Delta\underline{\mathbf{M}} := \Delta\underline{\mathbf{M}}^{self} \oplus \Delta\underline{\mathbf{M}}^{ngbr} \tag{3}$$

where $\Delta\underline{\mathbf{M}}^{self}$ measures self variation and $\Delta\underline{\mathbf{M}}^{ngbr}$ measures neighbor effects. $\Delta\underline{\mathbf{M}}^{ngbr}$ is further subdivided as the prediction from $\underline{\mathbf{N}}$ $Pred(\Delta\underline{\mathbf{M}}^{ngbr})$, and the neighbor residue, $\Delta\underline{\mathbf{M}}^{ngbr} \ominus Pred(\Delta\underline{\mathbf{M}}^{ngbr})$.

We make two assumptions in our approach. First, within each object, the self variations $\{\Delta\underline{\mathbf{M}}^{self}\}$ and the residues from the predictions $\{\Delta\underline{\mathbf{M}}^{ngbr} \ominus Pred(\Delta\underline{\mathbf{M}}^{ngbr})\}$ are considered to be statistically uncorrelated. Second, we assume that the effect of the neighboring objects is local. Based on the second assumption we define the sets $\underline{\mathbf{N}}$, $\underline{\mathbf{A}}$, and hence $\underline{\mathbf{U}}$. We currently choose atoms in the two sets based on Euclidean distance between atoms in nearby objects. $\Delta\underline{\mathbf{N}}$, $\Delta\underline{\mathbf{A}}$, and $\Delta\underline{\mathbf{U}}$ denote the m-rep variations in the sets $\underline{\mathbf{N}}$, $\underline{\mathbf{A}}$, and $\underline{\mathbf{U}}$ respectively.

3.1 Iterative steps

In calculating the geometric statistics, we begin with a simple assumption on the separation of each object's $\Delta\underline{\mathbf{M}}$ into self and neighbor components and then refine that separation by repeating the following steps over all figures in the multi-object m-reps.

In the following description of the estimation of the statistics for an object, the index over the objects and the index over the training cases is skipped.

Self step. We do PGA on $\Delta\underline{\mathbf{M}} \ominus \widehat{\Delta\underline{\mathbf{M}}}^{ngbr}$ which gives the shape space and estimate of the self part of each training case $\widehat{\Delta\underline{\mathbf{M}}}^{self}$. The hat $\widehat{(\cdot)}$ indicates the best estimate of either neighbor or self components up to the previous iteration.

Neighbor step.

1) Augmentation. We first subtract the estimate of the self part from each training case because we do not want to corrupt the effect from the neighbor by the effect to other neighboring objects from the object, i.e.,

$$\Delta\underline{\mathbf{A}}^{ngbr} := \Delta\underline{\mathbf{A}} \ominus \widehat{\Delta\underline{\mathbf{A}}}^{self}. \tag{4}$$

Then, because we need to predict $\Delta\underline{\mathbf{A}}^{ngbr}$ based on $\widehat{\Delta\underline{\mathbf{N}}}^{self}$, we form an augmented set of differences:

$$\Delta\underline{\mathbf{U}} := \Delta\underline{\mathbf{A}}^{ngbr} \cup \widehat{\Delta\underline{\mathbf{N}}}^{self}. \tag{5}$$

We use $\Delta\underline{\mathbf{N}}^{self}$ rather than $\Delta\underline{\mathbf{N}}$ because our initial assumption of local effect leads to $\Delta\underline{\mathbf{A}}^{ngbr}$ of the object and $\Delta\underline{\mathbf{N}}^{ngbr}$ of its neighbors being statistically independent.

2) Prediction. (1) Predictor function: We perform PGA on $\Delta\underline{\mathbf{U}}$ to find the shape space of the augmented atoms $\Delta\underline{\mathbf{U}}$. The shape space is used to find the deterministic effect from the neighbors as follows.

$$Proj(\Delta\underline{\mathbf{A}}^{ngbr}) = \exp_\mu\left(\sum_{l=1}\langle\log_\mu(\widehat{\Delta\underline{\mathbf{N}}}^{self}), v_l\rangle \cdot v_l\right), \tag{6}$$

$$Pred(\Delta\underline{\mathbf{A}}^{ngbr}) := Proj(\Delta\underline{\mathbf{A}}^{ngbr}) \tag{7}$$

where $\{v_l\}_{l=1}$ are principal directions in the tangent space of $\Delta\underline{\mathbf{U}}$ at its mean μ. Note that $\widehat{\Delta\underline{\mathbf{N}}}^{self}$ means $\mu|_{\underline{\mathbf{A}}}\cup\widehat{\Delta\underline{\mathbf{N}}}^{self}$ implicitly when $\log_\mu(\cdot)$ is applied.[1]

(2) Updated augmented set: We now form a newly updated augmented set after removing the prediction from the residue from the self estimate.

$$\Delta\underline{\mathbf{A}}^{rmdr} = \Delta\underline{\mathbf{A}}^{ngbr} \ominus Pred(\Delta\underline{\mathbf{A}}^{ngbr}), \tag{8}$$

$$\Delta\underline{\mathbf{U}}' := \Delta\underline{\mathbf{A}}^{rmdr} \cup \widehat{\Delta\underline{\mathbf{N}}}^{self}. \tag{9}$$

We then do PGA on the new augmented set $\Delta\underline{\mathbf{U}}'$ to obtain the shape space and the estimate $\widehat{\Delta\underline{\mathbf{A}}}^{ngbr}$ of the neighbor part of each training case. As a result, the estimate of the neighbor part comprises the two components: prediction and the estimate of the variation from the prediction.

$$\widehat{\Delta\underline{\mathbf{A}}}^{ngbr} = Pred(\Delta\underline{\mathbf{A}}^{ngbr}) \oplus \exp_\mu\left(\sum_{k=1}\langle\log_\mu(\Delta\underline{\mathbf{A}}^{rmdr}), v_k\rangle \cdot v_k\right). \tag{10}$$

3.2 Joint probability of interaction among objects

Using the joint probability on this decomposition of self and neighbor effects of multiple objects, we can interpret the prediction as the conditional mean assuming a Gaussian probability distribution. This interpretation is valid as long as we can show that the following conditions hold: the self effect and neighbor effect within each object, neighbor effects among objects, and self effects among objects are independent.

To show this, we decompose the joint probability of multiple objects using conditional probability:

$$p(\{\underline{\mathbf{M}}_k\}) = p(\underline{\mathbf{M}}_k \mid \{\underline{\mathbf{M}}_j | j \neq k\}) \, p(\{\underline{\mathbf{M}}_j | j \neq k\}), \tag{11}$$

where k goes over the number of objects. Moreover,

$$p(\underline{\mathbf{M}}_k \mid \{\underline{\mathbf{M}}_j | j \neq k\}) = p(\underline{\mathbf{M}}_k^{self}, \underline{\mathbf{M}}_k^{ngbr} \mid \{\underline{\mathbf{M}}_j^{self}, \underline{\mathbf{M}}_j^{ngbr} | j \neq k\}). \tag{12}$$

---

[1] Refer to [4] for detailed explanation of the log map and the exponential map.

Since we have assumed the locality of the effect of the neighboring objects and we choose $\underline{\mathbf{N}}$ as a set of medial atoms in neighboring objects that has influence on the variation of the shape of an object, we can replace the set of atoms in $\{\underline{\mathbf{M}}_j^{self}, \underline{\mathbf{M}}_j^{ngbr} | j \neq k\}$ with $\underline{\mathbf{N}}$. If the independence conditions stated above hold, then we can further simplify the joint probability distribution as follows:

$$p(\underline{\mathbf{M}}_k^{self}, \underline{\mathbf{M}}_k^{ngbr} \mid \underline{\mathbf{N}}_k^{self}) = p(\underline{\mathbf{M}}_k^{self}) \, p(\underline{\mathbf{M}}_k^{ngbr} \mid \underline{\mathbf{N}}_k^{self}). \qquad (13)$$

4 Application on male-pelvis model and results

4.1 Materials

The training models were obtained from male-pelvis CT images of real patients taken over a series of days who underwent radiotherapy treatment. Three organs, namely the bladder, prostate, and a section of the rectum that is adjacent to the prostate are modelled. Both ends of the rectum model are arbitrary. A clinician contoured each organ slice by slice to generate binary images for all three organs. A single-figure m-rep was then fit to bladder, prostate, and rectum separately in binary images: 5×6 grids of medial atoms for the bladder, 7×4 grids of medial atoms for the prostate, and 15×3 grids of medial atoms for the rectum are used. We have software developed to fit a single figure m-rep to binary image that prevents penetration among fitted m-reps, prevents folding of the interior of the object represented, and maintains regularity of grid across the cases for correspondence of medial atoms [14]. We aligned the fitted three m-reps for bladder, prostate, and rectum of each patient by a similarity transformation that is computed from two landmarks, at the apex and base of the prostate landmark. Then those aligned m-reps for bladder, prostate, and rectum are combined into one ensemble m-rep. The total number of medial atoms are 103, and the number of parameters in the ensemble m-rep is 927.

4.2 Application of probability density estimation to male-pelvis model

We have applied our approach to male-pelvis models of five patients m-rep fits of which were obtained as described in the previous section. Patients are numbered as 3101, 3106, 3108, 3109, and B163. We have 14 m-rep fits for 3101, 17 for 3106, 18 for 3108, 18 for 3109, and 15 for B163. Models fitted to the first treatment image are used as the reference model from which the variation of the rest of models are taken.

In the first iteration, since we know that the self part of the bladder and rectum changes dominate the neighbor parts, we assume that the neighbor parts in variations of the bladder and rectum are zero. Similarly, we set the self part in the prostate to zero, for the shape of prostate changes little except as affected by the bladder and rectum.

Starting with $\Delta\underline{\mathbf{M}}_b$, $\Delta\underline{\mathbf{U}}_b$, $\Delta\underline{\mathbf{M}}_p$, $\Delta\underline{\mathbf{U}}_p$, $\Delta\underline{\mathbf{M}}_r$, $\Delta\underline{\mathbf{U}}_r$ where subscript b, p, r represent bladder, prostate, and rectum respectively, the order we compute

patient	total variation per object					
patient no.	bladder self	bladder neighbor	rectum self	rectum neighbor	prostate neighbor	prostate self
3101	0.379383	0.014782	0.360542	0.004983	0.179949	0.006880
3106	0.082828	0.002576	0.102897	0.001188	0.031047	0.003648
3108	0.391689	0.010346	0.181145	0.012492	0.135748	0.009021
3109	0.080293	0.006388	0.132851	0.003501	0.043438	0.005439
B163	0.067945	0.002470	0.137690	0.002819	0.053831	0.003205

Table 1. Total variations of two effects, self, and neighbor per organ that are estimated after 2nd iteration

the estimate of neighbor and self effect in each organ in the first iteration is as follows.

1. Self effect on bladder, and rectum differences $\Delta\underline{\mathbf{M}}_b$, $\Delta\underline{\mathbf{M}}_r$, assuming $\Delta\underline{\mathbf{M}}_b^{ngbr}$, $\Delta\underline{\mathbf{M}}_r^{ngbr}$ are zero
2. Neighbor effect on prostate differences $\Delta\underline{\mathbf{U}}_p$, assuming $\Delta\underline{\mathbf{A}}_p^{self}$ are zero. Note that we use for prediction the estimate of the self variations of bladder and rectum from step 1.
3. Self effect on prostate residue from the estimate of the neighbor effect. The residue is $\Delta\underline{\mathbf{M}}_p^{self} := \Delta\underline{\mathbf{M}}_p \ominus \widehat{\Delta\underline{\mathbf{M}}}_p^{ngbr}$.
4. Neighbor effect on bladder and rectum residue from the estimate of the self effect $\Delta\underline{\mathbf{U}}_b$, $\Delta\underline{\mathbf{U}}_r$ where $\Delta\underline{\mathbf{A}}_b := \Delta\underline{\mathbf{A}}_b \ominus \widehat{\Delta\underline{\mathbf{A}}}_b^{self}$ and $\Delta\underline{\mathbf{A}}_r := \Delta\underline{\mathbf{A}}_r \ominus \widehat{\Delta\underline{\mathbf{A}}}_r^{self}$. We again use the estimate of the self part of the prostate $\widehat{\Delta\underline{\mathbf{M}}}_p^{self}$ from step 3 to compute the prediction of bladder and rectum from change of their neighboring object prostate.

For the later iterations, we repeat the steps described in section 3.1 with the updated estimates of self and neighbor effects from the previous iteration.

4.3 Result

Table 1 compares the estimates of total variations of the two effects for each organ after the 2nd iteration. They are the sum of eigenvalues that are estimated in each step described in the previous section. Figure 1 shows the primary mode of self variation of the bladder and the associated prediction of the deformation of the prostate in the patient B163. We can see a dent formed in the bladder in which the prostate fits as the bladder fills.

5 Discussion and conclusion

The results are consistent with what we know about the anatomy and see in the data. The self terms for the bladder and rectum dominate the neighbor terms,
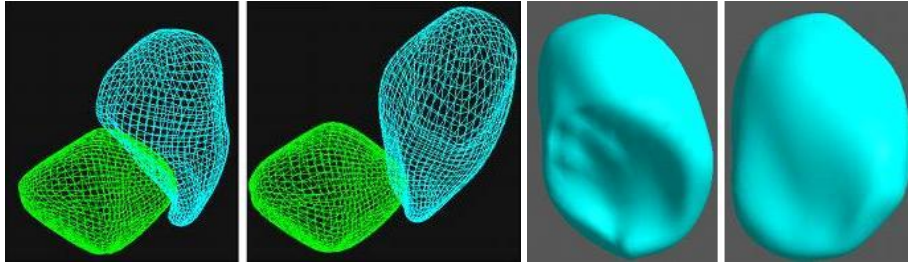
Fig. 1. These 4 figures show the prediction of the deformation on the prostate brought by the change of the patient B163. The two objects in the left 2 panels are the bladder (cyan) and the prostate (green) in wire frame and the right 2 panels show separately the bladder of the left 2 panels in solid. The bladder in the right 2 panels is in 2 standard deviations from the mean for a principal modes of the self effect estimated in the bladder. The left 2 panels show the predicted prostate corresponding to the two positions of the bladder shown in the right 2 panels.

reflecting the fact that these organs' variations are principally due to changes in their contents. On the other hand, the neighbor term for the prostate dominates the self term, reflecting the fact that the prostate is a rather hard organ that is pushed upon by the rectum and bladder.

Moreover, the predictions of the prostate from the bladder and the rectum seem realistic. Also, the prostate changes from its prediction are smaller than the self changes in the bladder and rectum, which are known to be larger.

The bladder self changes include modes corresponding to lengthening, widening, and lapping around the prostate, all anatomically observed processes. Also encouraging is that the prostate predictions of the bladder self modes have the prostate following the change in the indentations of the bladder while keeping the prostate almost entirely nonintersecting. Furthermore, the prostate self modes also make consistent predictions on the bladder indentation.

While this experiment is limited, it suggests that our new approach to separate out inherent variation of an object itself and effects from its neighboring objects is fruitful.

We still need to do further analysis to verify that our estimates truly reflects the self and neighbor effects of multi-objects. We plan to determine what are self and neighbor effects by simulating the obvious neighbor effects and self effects independent from neighbor effects on an ensemble of multiple ellipsoids m-reps and apply our approach on the the simulated ensembles.

We will also incorporate the new geometric statistics of the male pelvic organs as the prior within our segmentation method's posterior objective function and evaluate this prior by the effectiveness of the segmentation of these organs.

An open issue is how to choose augmented atoms. Clearly, that choice affects our estimate of self and neighbor effects. We believe that we should choose the most highly correlated atoms with those in the target object. In separate research

we are measuring this correlation, and the results of that research will provide us a firmer basis for our choice than the distance criterion presently used.

In the nonlinear manifold on which m-reps are situated, addition operations is not commutative. The separation of $\Delta\underline{\mathbf{M}}$ into $\Delta\underline{\mathbf{M}}^{self} \oplus \Delta\underline{\mathbf{M}}^{ngbr}$ is thus not equivalent to $\Delta\underline{\mathbf{M}}^{ngbr} \oplus \Delta\underline{\mathbf{M}}^{self}$. In our iterative algorithm, this non-commutativity is ignored and $\Delta\underline{\mathbf{M}}^{self}$, $\Delta\underline{\mathbf{M}}^{ngbr}$ are treated as if they are interchangeable. We must test whether the effect of our method's assumption of commutativity is significant.

We also need to test the four conditions stated in 3.2 to show our interpretation on joint probability holds.

6   Acknowledgements

References

1. Pizer, S., Fletcher, T., Fridman, Y., Fritsch, D., Gash, A., Glotzer, J., Joshi, S., Thall, A., Tracton, G., Yushkevich, P., Chaney, E.: Deformable m-reps for 3d medical image segmentation. International Journal of Computer Vision - Special UNC-MIDAG issue, (O. Faugeras, K. Ikeuchi, and J. Ponce, eds.) **55**(2) (2003) 85–106
2. Pilgram, R., Fletcher, P., Pizer, S., Pachinger, O., Schubert, R.: Common shape model and inter-individual variations of the heart using medial representation. submitted to IEEE TMI (2004)
3. Ray, S., Simpson, S., Muller, K.: (Structural covariance for multi-object image segmentation)
4. Fletcher, P.T., Lu, C., Pizer, S.M., Joshi, S.: Principal geodesic analysis for the study of nonlinear statistics of shape. IEEE Transactions on Medical Imaging **23**(8) (2004) 995–1005
5. Pizer, S., Jeong, J.Y., Lu, C., Muller, K., Joshi, S.: Estimating the statistics of multi-object anatomic geometry using inter-object relationships. In: in International Workshop on Deep Structure, Singularities and Computer Vision (DSSCV), (O.F. Olsen, L. Florack, and A. Kuijper, eds.). (2005) 60–71
6. Cootes, T., Taylor, C., Cooper, D., Graham, J.: Active shape models their training and application. Computer Vision and Image Understanding **61**(1) (1995) 38–59
7. Joshi, S.: Large Deformation Diffeomorphisms and Gaussian Random Fields for Statistical Characterization of Brain SubManifolds. PhD thesis, Dept. of Electrical Engineering, Sever Institute of Technology, Washington Univ. (1997)
8. Tsai, A., Yezzi, A., Wells, W., Tempany, C., Tucker, D., Fan, A., Grimson, E., Willsky, A.: A shape-based approach to curve evolution for segmentation of medical imagery. IEEE Transactions on Medical Imaging **22**(2) (2003) 137–153

10

9. Vaillant, M., Davatizikos, C.: Hierarchical matching of cortical features for deformable brain image registration. In: Information Processing in Medical Imaging (IPMI). (1999) 182–195
10. Kapur, T., Beardsley, P., Gibson, S., Grimson, W., Wells, W.: Model based segmentation of clinical knee mri. In: Model-based 3D Image Analysis workshop (in conjuction with ICCV). (1998) 156–162
11. Davatzikos, C., Xiaodong, T., Shen, D.: Hierarchical active shape models, using the wavelet transform. IEEE Transactions on Medical Imaging **22**(3) (2003) 414–423
12. Pohl, K., Fisher, J., Levitt, J., Shenton, M., Kikinis, R., Grimson, W., Wells, W.: A unifying approach to registration, segmentation, and intensity correction. In: Medical Image Computing and Computer Assisted-Intervention. (2005) 310–318
13. Lu, C., Pizer, S., Joshi, S., Jeong, J.Y.: Statistical multi-object shape models. Technical report, UNC Chapel-Hill (2005)
14. Merck, D., Tracton, G., Saboo, R., Chaney, E., Pizer, S., Joshi, S.: A methodology and implementation for constructing geometric priors for deformable shape models (2006) in Conference submission.